Journal of Computational Design and Engineering, Vol. 1, No. 1 (2014) 48~54
www.jcde.org

Automatic detection of the optimal ejecting direction based on a discrete Gauss map

Masatomo Inui, Hidekazu Kamei and Nobuyuki Umezu*

Department of Intelligent Systems Engineering, Ibaraki University, 4-12-1 Nakanarusawa, Hitachi, Ibaraki, Japan

(Manuscript Received September 14, 2013; Revised October 24, 2013; Accepted November 1, 2013)

Abstract

In this paper, the authors propose a system for assisting mold designers of plastic parts. With a CAD model of a part, the system automatically determines the optimal ejecting direction of the part with minimum undercuts. Since plastic parts are generally very thin, many rib features are placed on the inner side of the part to give sufficient structural strength. Our system extracts the rib features from the CAD model of the part, and determines the possible ejecting directions based on the geometric properties of the features. The system then selects the optimal direction with minimum undercuts. Possible ejecting directions are represented as discrete points on a Gauss map. Our new point distribution method for the Gauss map is based on the concept of the architectural geodesic dome. A hierarchical structure is also introduced in the point distribution, with a higher level "rough" Gauss map with rather sparse point distribution and another lower level "fine" Gauss map with much denser point distribution. A system is implemented and computational experiments are performed. Our system requires less than 10 seconds to determine the optimal ejecting direction of a CAD model with more than 1 million polygons.

Keywords: Ejecting direction; Undercut detection; Injection molding; Feature recognition; Concurrent engineering; CAD

1. Introduction

Most plastic parts for consumer products are produced by injection molding. With this method, the molded part must be removed from the mold core in a single ejecting direction. In order to realize the smooth removal, the part should be designed such that it does not have any "undercuts" in the ejecting direction; otherwise, expensive sliding core mechanisms are necessary. Figure 1 illustrates an example of undercuts. Since concave shapes on the part interfere with the mold, the formed part cannot be removed from the mold in any direction (see Figure 1(a)). By using the sliding core mechanisms, the interfering portions on the core and cavity are resolved (see Figure 1(b)) and the molded part can be smoothly ejected.

A reduction of the number of component parts is a basic strategy to design a product with low production cost [1]. When using this strategy, more functions are expected on a single part; therefore, the part shape tends to be complex and it often has many undercuts. After the part is designed, mold engineers spend much time designing injection molds with many sliding cores in order to resolve the undercuts.

In this paper, a system is proposed to assist the mold designer of plastic parts that have sliding core mechanisms. Supplied with a CAD model of a part, the system automatically determines the optimal ejecting direction of the part with the minimum number, minimum area, or minimum

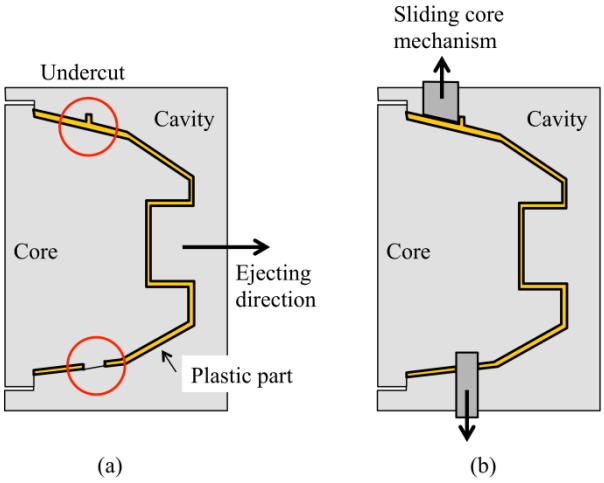

Figure 1. (a) Core and cavity with two undercuts, (b) examples of sliding core mechanism for resolving the undercuts.

*Corresponding author. Tel.: +81-294-38-5262 , Fax.: +81-294-38-5229
E-mail address: umezu@mx.ibaraki.ac.jp

doi : 10.7315/JCDE.2014.005

Figure 2. Rib features placed on a plastic part.

volume of the undercuts. Since plastic parts are generally very thin, many rib features are placed on the inner side of the part to give sufficient structural strength, as shown in Figure 2. Each rib feature strictly constrains the possible ejecting direction. Our system extracts rib features from the CAD model of the part, and derives the possible ejecting directions based on the geometric properties of the extracted features. It then selects the optimal direction with the minimum number of undercuts. Our system is not applicable for parts that have no rib features. This limitation does not reduce the practical value of the method because such parts without rib features are generally very small and of a simple shape, and the molding engineers can design a cavity and core for the part without any difficulty.

The system uses a discrete representation of the Gauss map [2] for recording the candidate ejecting directions, where each direction corresponds to a point on a unit sphere. Points (= candidate directions) are not uniformly distributed on the sphere based on the equal angular interval in the spherical coordinate system. More points are placed in the region near the north and south poles. On the other hand, fewer points are given in the zone near the equator line, which decreases computation accuracy. Our new point distribution method for the discrete Gauss map is based on the concept of the architectural geodesic dome. This method can locate points on the unit sphere in a constant density. A hierarchical structure is also introduced in the point distribution, with a higher level "rough" Gauss map with sparse point distribution and another lower level "fine" Gauss map with a much denser point distribution.

An algorithm based on this structure is developed to select the optimal ejecting direction. In the first step, a rough Gauss map with sparse point distribution is used to select the optimal ejecting direction. The fine Gauss map with dense point distribution is then used to accurately determine the optimal direction around the initial solution. Our system requires less than 10 seconds to determine the optimal ejecting direction of a CAD model with more than 1 million polygons.

The organization of this paper is as follows. In Section 2, the related studies are briefly reviewed. The basic processing flow of our rib-feature-based ejecting direction determination algorithm is explained in Section 3. Details of the algorithm are given in Section 4, as well as an explanation of the performance improvements obtained by introducing the discrete and hierarchical Gauss map representations. In Section 5, experimental results of the automatic determination of the optimal ejecting direction are illustrated.

2. Related studies

The undercut detection and the selection of the undercut free ejecting direction of plastic parts are interesting research topics and many research works have been carried out in the CAD field. Priyadrashi and Gupta proposed an algorithm for detecting undercuts of a part ejected in a specific parting direction [3]. They used the graphics hardware function for accelerating the detection algorithm [4]. However, their method is not applicable for selecting the optimal ejecting direction.

Wuerger and Gadh proposed an algorithm for automatically selecting the undercut free ejecting direction based on the CAD model of the part [5]. In their subsequent paper, this method is extended to handle rotational ejection [6]. Since their works are theoretical, several imaginary applications of the algorithm are only given for very simple examples. The applicability of the method to real plastic parts with complex shapes is not evaluated.

Khardekar et al. proposed two methods for automatically determining the undercut free ejecting directions from a polygonal CAD model [7]. Unlike [5] and [6], they implemented working systems and applied them to several CAD models to verify their practical applicability. Although they introduced the parallel processing capability of GPU to accelerate the systems, they still require 10 minutes to determine the possible ejecting direction for a simple part with several thousand polygons. These studies focused on the automatic detection of the undercut free ejecting direction. Most actual plastic parts currently used in practice have very complex shapes and are not free of undercuts. The methods proposed in [5], [6], and [7] are not applicable for such parts and therefore cannot assist the designers.

Chen et al. proposed an algorithm applicable to a part with undercuts [8]. In their method, "pocket" shapes are extracted using the difference between the convex hull of the part and the original part shape. The visibility maps of the pockets are mapped on a unit sphere. The optimal ejecting direction with the minimum number of undercuts is determined by finding a pair of antipodal points located on the maximum number of visibility maps. Chen et al. extended this idea by using two levels of visibility for determining the ejecting direction [9]. With the same visibility map concept, Nee et al. determined the optimal ejecting direction as the direction with the minimum undercut volume [10, 11].

In contrast to the theoretical works carried out by Chen et

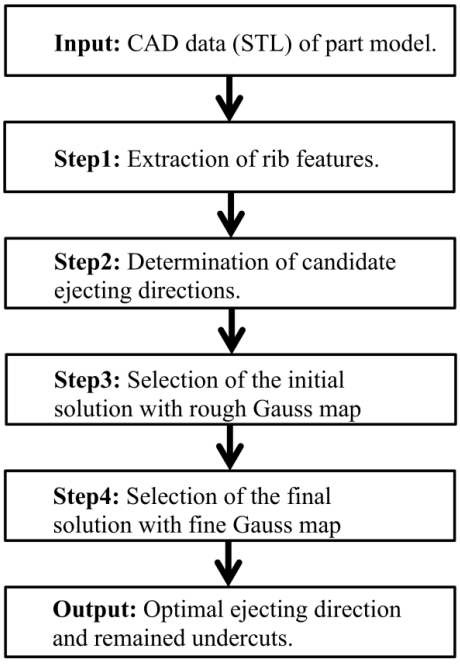

Figure 3. Input, output, and processing flow of the proposed algorithm.

al. and Nee et al., in this present study, the authors focused on reducing the computation time required for obtaining the optimal ejecting direction, which is one of the most important factors when using the system in practice. Our method uses the rib features on the plastic part to reduce the number of possible ejecting directions. The rib features are automatically extracted from the polygonal CAD model of the part. The feature recognition of the mechanical part was actively studied in the 1990s [12, 13]. In this paper, a type of rule based recognition method specialized for the rib feature is used.

3. Algorithm outline

3.1 Input and output

Our system requires a CAD model of a plastic part as an input. It is assumed that the model shape is represented as a set of triangular polygons, such as in the STL format. After the computation, the system displays the optimal ejecting direction with the minimum undercuts. It also visualizes the undercut shape in the derived ejecting direction.

3.2 Processing flow

Many rib features are placed on the surface to give sufficient strength to the plastic part. The ejecting direction of the part is selected so that the rib features do not produce any undercuts; otherwise, the designer must define a large number of sliding mechanisms for the ribs, which is practically impossible.

According to the concept mentioned above, our algorithm finds the optimal ejecting direction using the following four steps (see Figure 3).

Step 1: Extraction of rib features. Rib features are extracted from the polygonal model of the plastic part by using a rule based extraction algorithm developed for the authors' prior system [14].

Step 2: Determination of candidate ejecting directions. For each rib feature, possible ejecting directions based on the geometric property of the feature are mapped to the rough Gauss map by using the method given in [6]. This process is repeated for all rib features and the intersection of the mapped directions is used as the candidates of the optimal ejecting directions.

Step 3: Selection of the initial solution with rough Gauss map. For each candidate direction given in the rough Gauss map, the undercut shapes on the part's surface in the ejecting process are detected. According to the user's selection, the number of undercuts, the total surface area of the undercuts, or the total volume of the undercuts is evaluated and one ejecting direction with the minimum undercut number/area/volume is returned as the initial solution.

Step 4: Selection of the final solution with fine Gauss map. The direction obtained in Step 3 has a corresponding point in the rough Gauss map. A small rectangular area around the point is projected to the fine Gauss map, and ejecting directions near the initial solution are selected from the fine Gauss map as new candidates for the optimal direction. For each candidate direction, the undercut shapes are evaluated again and the final optimal direction is determined.

4. Details of the algorithm

4.1 Extraction of rib features

Our system extracts the rib features from the CAD model of the part as a set of four polygons satisfying the following geometric relationships.

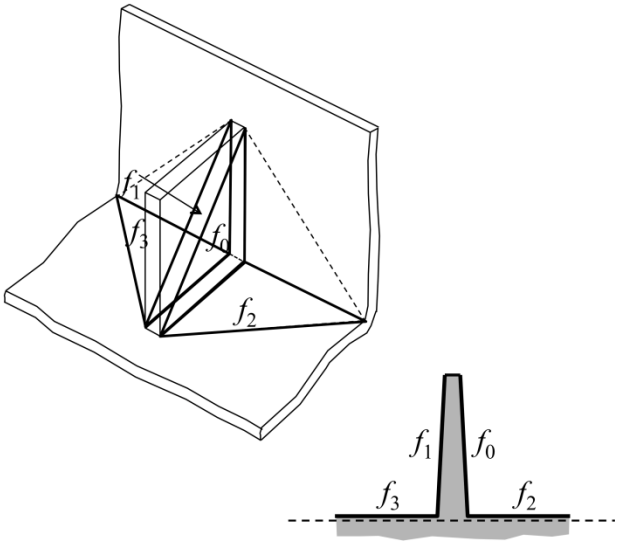

Figure 4. Rib feature with four polygons.

- 2 polygons (polygons f_0 and f_1 in Figure 4) are almost parallel and their normals are in mutually opposite directions. In addition, their distances are sufficiently small (generally less than 2mm).
- 2 polygons (polygons f_2 and f_3 in Figure 4) are located on the same plane, or very close to it, and are adjacent to f_0 and f_1 respectively, while being almost perpendicular to polygon f_0 and f_1.

Our current implementation executes the exhaustive search for all polygons on the model to determine sets of 4 polygons that satisfy the above conditions. Since component polygons of one rib feature must exist in a limited spatial region, localization techniques are helpful for reducing the cost of the feature extraction. The authors are now introducing a spatial grid structure that tightly holds the model for localizing the search area. Preliminary experiments show a promising result and it will be implemented in the system.

4.2 Determination of candidate ejecting directions

Consider a point $\boldsymbol{p}$ on one polygon f of a rib feature. $\boldsymbol{p}$ can move in all directions that do not point into the object. Such directions are used to organize a hemisphere on the Gauss map where the dividing circle is a set of vectors that are perpendicular to the normal vector of f. The hemisphere represents the possible ejecting directions of any points on a polygon f (see Figure 5). A rib feature can be recognized as a combination of two concave shapes (f_0–f_2 and f_1–f_3 in Figure 4). The intersection of the component polygon's hemisphere represents the possible ejecting direction for each concave shape. E_0 and E_1 in Figure 6 represent the ejecting directions of f_0–f_2 and f_1–f_3, respectively.

Ejecting direction E_0 on the Gauss map only represents the possible motions of the mold-half that touch the concave shape f_0–f_2. It is assumed that the other mold-half moves simultaneously in the opposite direction. E_2, a mirror shape of E_0, thus also corresponds to the possible ejecting direction.

The result of the ejecting directions for the concave shape becomes the union of E_0 and E_2 as shown in Figure 6. The ejecting direction for the concave shape f_1–f_3 is similarly defined as the union of E_1 and E_3.

The ejecting direction for a single rib feature is finally obtained as the intersection of the ejecting directions for its two component concave shapes. The direction has a combined shape of a vertical thin ring and a horizontal circle as shown in Figure 6. This computation is repeatedly executed for all rib features extracted on the part, and the intersection of all ring-circle shapes on the Gauss map finally forms the range of possible ejecting directions for the part.

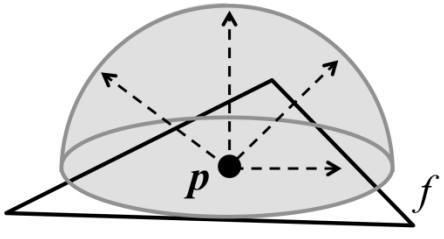

Figure 5. Ejecting directions of a point p on a polygon f.

In the above method, the intersection and union of the curved figures on the Gauss map are frequently calculated. In our implementation, a discrete and hierarchical representation of the Gauss map is adopted for fast and stable computation. In this method, a Gauss map is represented with points uniformly distributed on the unit sphere. A Boolean flag is specified at each point to distinguish whether or not the point is located inside the figure. The intersection of the two figures A and B on the discrete Gauss map is achieved by selecting points that are inside both A and B. The union of the figures is computed in a similar manner by selecting the points which are located inside A or B.

As a point distribution method for a discrete Gauss map, an algorithm based on the geodesic dome structure is adopted. A geodesic dome is a spherical structure wrapped with triangles of approximately the same size. This structure is typically used in radar domes. The construction of a geodesic dome starts with an icosahedron inscribed in a sphere. Each triangle of the icosahedron is tiled into four small triangles of uniform size, and the vertices of the tiles are projected onto the sphere. This tiling and projecting process is iterated until a tiled sphere with sufficiently small triangles is obtained. The verti-

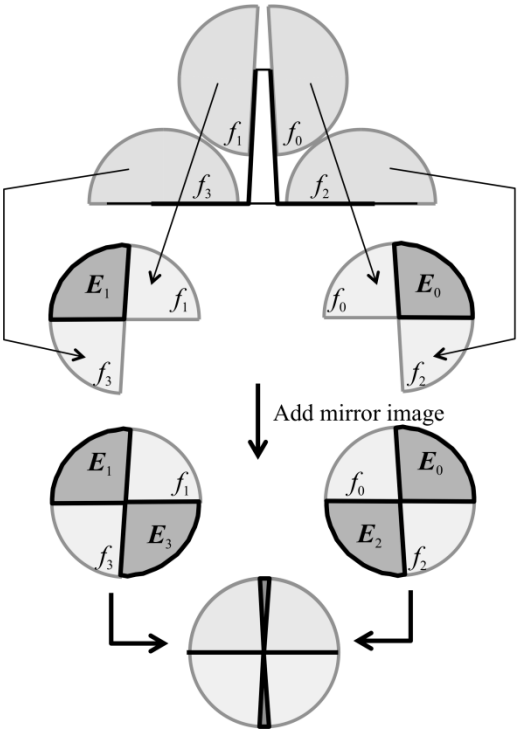

Figure 6. Possible ejecting directions for a rib with f_0, f_1, f_2, and f_3 on the Gauss map.

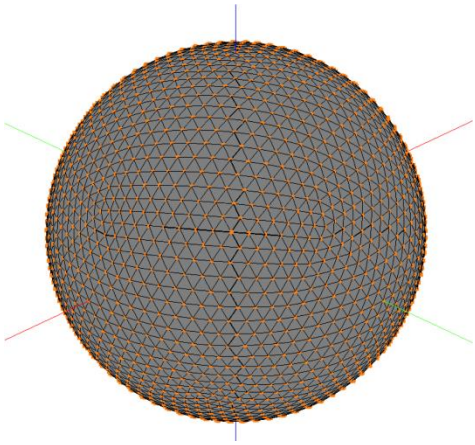

Figure 7. Rough Gauss map based on a geodesic dome.

ces of the covering triangles are used as the discrete Gauss map. In our system, a rough Gauss map is defined using a geodesic dome as shown in Figure 7. This dome structure is obtained by iterating the tiling operation until the angular length of each edge of triangles becomes 4.5 degrees. The candidate ejecting directions obtained in Step 2 are represented as points with a true flag on the rough Gauss map.

4.3 Selection of the initial solution with rough Gauss map

For each candidate direction obtained in Step 2, the undercut detection with the depth peeling technique [15] is executed to compute the position, area, and volume of the undercut. Depth peeling is an extensive use of the depth buffer method, a well-known computer graphics technique for eliminating the hidden surfaces of objects. Figure 8 illustrates the depth peeling process of a part, viewed in the opposite direction of the ejecting direction, using the orthogonal projection method.

By using the depth buffer mechanism, the points on the surface closest to the viewer (points on solid red curve) are selected and their image is rendered on the frame buffer. After the rendering, the location (depth) data of the selected points are transferred from the depth buffer to a depth texture, and the second rendering operation is executed. In this process, the data in the depth texture is used as a filter, while only those points on the part surface that are farther than the depth data stored in the depth texture are rendered. As a result, the points on the surface that are second closest to the viewer (points on solid blue curve) are selected by the depth buffer for this time, and their image is rendered on the frame buffer. The operation mentioned above is repeated until all points on the part surface are rendered.

After the depth peeling, the points on the part surface are classified into groups according to the rendering times. As shown in Figure 8, the points appearing in the 2i surface where $i > 0$ and its opposite part on the 2i–1 surface correspond to the undercuts. In our current implementation, the user can select either the number, total area, or total volume

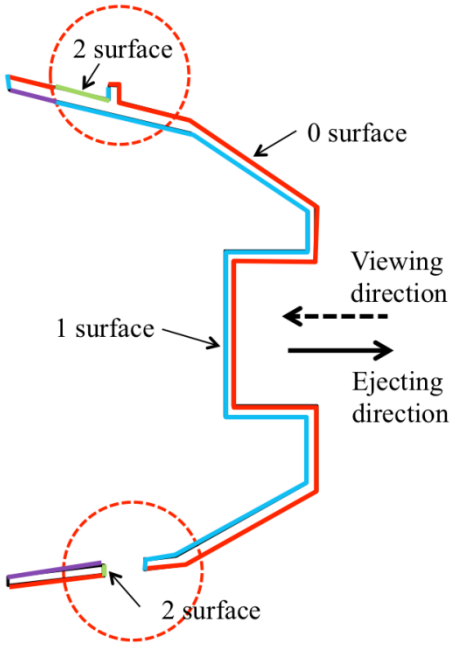

Figure 8. Results of the depth peeling operation.

of the undercuts as a measure for evaluating the optimality of the ejecting direction. According to the user selection, the system evaluates the number/area/volume of undercuts for each candidate direction in the following manner.

Number of undercuts: After the classification of the points on the surface, the points appearing on the 2i surface are grouped according to their connectivity, and the number of groups is returned as the number of undercut shapes. In the case shown in Figure 8, the number of undercut groups returned is 2.

Total area of the undercuts: The number of points appearing on the 2i surface and on the opposing 2i–1 surface is proportional to the area of the undercuts projected on a plane that is perpendicular to the ejecting direction. Instead of the true area, the total number of points on the undercut shape is returned as a reasonable approximation of the undercut area.

Total volume of the undercuts: Each point on the 2i surface, and its corresponding point on the 2i–1 surface, is connected by a short segment. After the connection, the length of the connecting segments is accumulated. Since the sum of the segment lengths is proportional to the total volume of undercut shapes, the sum is returned instead.

According to the user selection, the system evaluates the number/area/volume of undercuts for each candidate direction and returns the optimal direction with the minimum undercut as the initial solution.

4.4 Selection of the final solution with fine Gauss map

A fine Gauss map with a very dense point distribution is then defined by assigning grid points around the initial solution on the rough Gauss map. Figure 9 illustrates the point

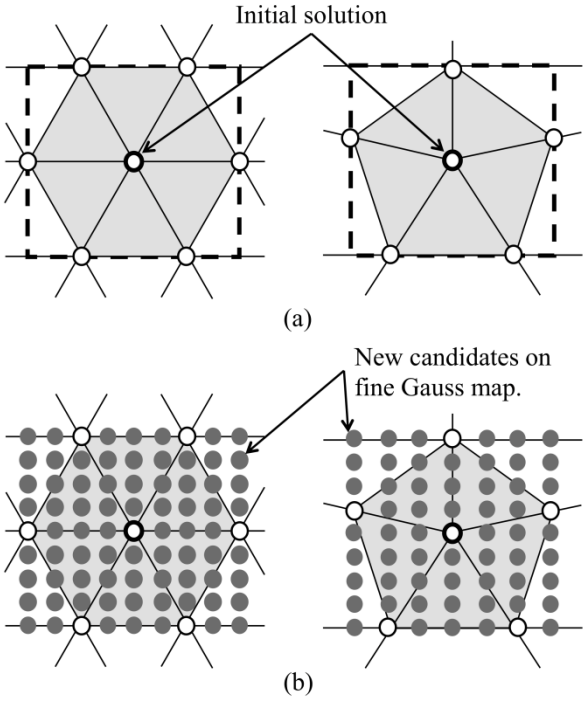

Figure 9. New candidate directions around the initial solution on the fine Gauss map.

selection method with the fine Gauss map. The initial solution obtained in Step 3 has a corresponding point on the rough Gauss map.

Using the geodesic structure of the rough Gauss map, a set of triangles adjacent to the point is obtained. The number of adjacent triangles equals to six or five. For either case, a bounding rectangle is defined on the sphere, as shown in Figure 9(a), and dense grid points are generated in the rectangle so that they are at equal angular intervals (see Figure 9(b)).

For each ejecting direction corresponding to the generated point, the number, total area, or total volume of the undercuts is evaluated again and the optimal direction is selected as the final solution. Undercuts corresponding to the optimal ejecting direction are visualized in the display to suggest the required shape and location of the sliding core mechanism.

5. Computational experiments

By using the technology mentioned above, the optimal ejecting direction determination system is implemented using Visual C++ and OpenGL, and computational experiments are performed. A PC with an Intel Core i7 Processor (3.4GHz), 4GB memory, and nVIDIA GeForce GTX-560 GPU is used in the experiments. Two sample CAD models are used for the performance evaluation.

The first model is illustrated in Figure 10. This part model is very finely tessellated to have 1,708,000 polygons. Our system is applied to this model for computing the optimal ejecting direction with the minimum number of undercuts.

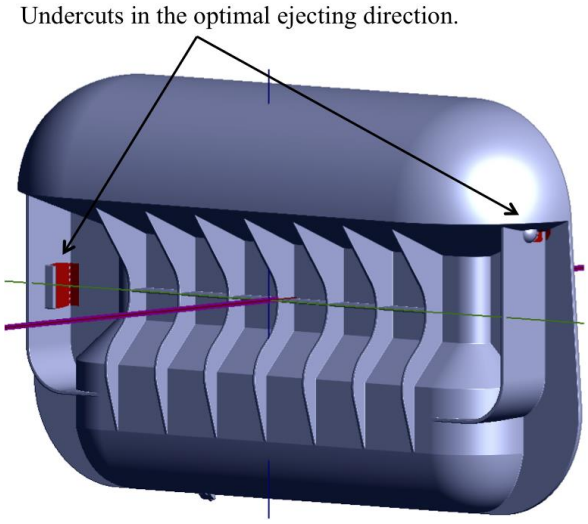

Figure 10. Optimal ejecting direction for a sample part with 1,708,000 polygons.

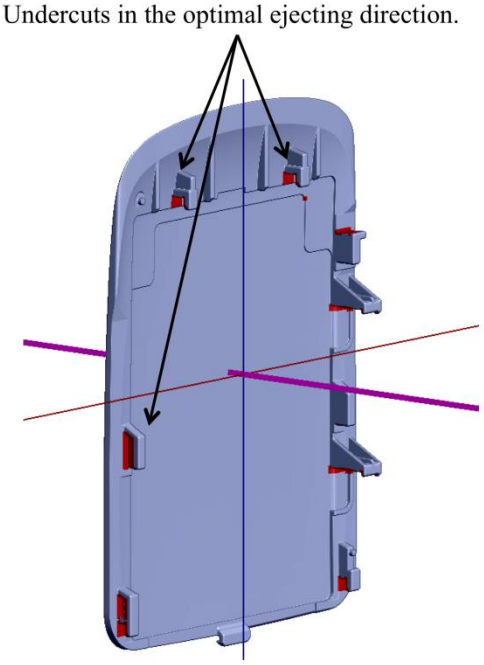

Figure 11. Optimal ejecting direction for a sample part with 51,928 polygons.

The ejecting direction parallel to the X-axis is selected as the optimal direction. A total of 8.96 seconds is required for the computation, including the rib features extraction, the candidate direction selection, and the optimal ejecting direction determination.

The second model is shown in Figure 11. This model has 51,928 polygons. Our system determines that the ejecting direction parallel to the Y-axis direction is the optimal direc-

tion with the minimum number of undercuts. 2.34 seconds is required to determine the optimal ejecting direction for this case.

6. Conclusions

In this paper, a method for automatically determining the optimal ejecting direction with minimum undercuts is proposed for assisting injection mold design. The proposed algorithm uses the rib structures on the part to reduce the number of possible ejecting directions. For each ejecting direction, the undercuts in the ejection process are evaluated, and the ejecting direction with the minimum number/area/volume of undercuts is returned as the optimal direction.

A new point distribution method for the discrete Gauss map is adopted which is based on the concept of the architectural geodesic dome. A hierarchical structure is also introduced in the point distribution, with a higher level "rough" Gauss map with sparse point distribution and another lower level "fine" Gauss map with much denser point distribution.

Our system is still at an experimental stage. The authors are now preparing a field test of the system in the actual mold design process. The proposed algorithm has been further improved basing on the suggestions and requests from the designers.

References

[1] Boothroyd G, Dewhurst R, Knight W. Product design for manufacture and assembly. New York (NY): Marcel Dekker; 1994. 540 p.

[2] Woo TC. Visibility maps and spherical algorithms. Computer-Aided Design. 1994; 26(1): 6-16.

[3] Priyadrashi AK, Gupta SK. Geometric algorithms for automated design of multi-piece permanent molds. Computer-Aided Design. 2004; 36(3): 241-260.

[4] Priyadrashi AK, Gupta SK. Finding mold-piece regions using computer graphics hardware. In: Proceedings of Geometric Modeling and Processing Conference; 2006 July 26-28; Pittsburgh, PA; p. 655-662.

[5] Wuerger D, Gadh R. Virtual prototyping of die design-theory and formulation. In: Proceedings of the Computer Aided Concurrent Design Symposium (ASME Design and Engineering Technical Conferences); 1995 Sep 17-20; Boston, MA; p.1001-1012.

[6] Kurth GR, Gadh R. Virtual prototyping of die-design: determination of die-open directions for near-net-shape manufactured parts with extruded or rotational features. Computer Integrated Manufacturing Systems. 1997; 10(1): 69-81.

[7] Khardekar R, Burton G, McMains S. Finding feasible mold parting directions using graphics hardware. In: ACM Symposium on Solid and Physical Modeling; 2005 June 13-15; Cambridge, MA; p. 233-243.

[8] Chen LL, Chou SY, Woo TC. Parting directions for mold and die design. Computer-Aided Design. 1993; 25(12): 762-768.

[9] Chen LL, Chou SY. Partial visibility for selecting a parting direction in mold and die design. Journal of Manufacturing Systems. 1995; 14(5): 319-330.

[10] Nee AYC, Fu MW, Fuh JYH, Lee KS, Zhang YF. Automatic determination of 3-d parting lines and surfaces in plastic injection mold design. Annals of the CIRP (College International pour la Recherche en Productique). 1998; 47(1): 95-98.

[11] Fu MW, Fuh JYH, Nee AYC. Undercut feature recognition in an injection mold design system. Computer-Aided Design. 1999; 31(12): 777-790.

[12] Gupta SK, Das D, Regli WC, Nau DS. Automated manufacturability analysis: a survey. Research in Engineering Design. 1997; 9(3): 168-190.

[13] Gupta SK, Nau DS. Systematic approach to analyzing the manufacturability of machined parts. Computer-Aided Design. 1995; 27(5): 323-342.

[14] Inui M, Kamei H, Umezu N. Automatic detection of ejecting direction of a part with minimum undercuts. In: Proceedings of Asian Conference on Designing and Digital Engineering (ACDDE); 2012 Dec 5-7; Niseko, Japan; Paper No.100017.

[15] Everitt C. Interactive order-independent transparency [Internet]. Santa Clara: nVIDIA; [cited 2013 Nov]. 11p. Available from: Everitt C. Interactive order-independent transparency [Internet]. Santa Clara: nVIDIA; [cited 2013 Nov]. 11p. Available from: https://developer.nvidia.com/content/interactive-order-independent-transparency